Toxicology in Vitro 82 (2022) 105383

Contents lists available at ScienceDirect

Toxicology in Vitro

journal homepage: www.elsevier.com/locate/toxinvit

Weak complex formation of adverse drug reaction-associated HLA—B57, B58, and B15 molecules

Tomohiro Shirayanagi [a], Akira Kazaoka [a], Kenji Watanabe [a], Liang Qu [b], Naoki Sakamoto [a], Tyuji Hoshino [b], Kousei Ito [a], Shigeki Aoki [a,*]

[a] Laboratory of Biopharmaceutics, Graduate School of Pharmaceutical Sciences, Chiba University, 1-8-1 Inohana, Chuo-ku, Chiba-city, Chiba 260-8675, Japan
[b] Department of Physical Chemistry, Graduate School of Pharmaceutical Sciences, Chiba University, 1-8-1 Inohana, Chuo-ku, Chiba-city, Chiba 260-8675, Japan

ARTICLE INFO

Editor: P Jennings

Keywords:
Human leukocyte antigen
β_2-microglobulin
Drug hypersensitivity
Molecular dynamics simulation

ABSTRACT

The combination of certain human leukocyte antigen (HLA) polymorphisms with administration of certain drugs shows a strong correlation with developing drug hypersensitivity. Examples of typical combinations are HLA-B*57:01 with abacavir and HLA-B*15:02 with carbamazepine. However, despite belonging to the same serotype, HLA-B*57:03 and HLA-B*15:01 are not associated with drug hypersensitivity. Recent studies have shown that several HLA polymorphisms are associated with multiple drugs rather than a single drug, all resulting in drug hypersensitivity. In this study, we compared the molecular structures and intracellular localization of HLA-B*57:01, HLA-B*58:01, and HLA-B*15:02, which pose risks for developing drug hypersensitivity, as well as HLA-B*57:03 and HLA-B*15:01 that do not present such risks. We found that HLA molecules posing risks have a low affinity for the subunit β_2-microglobulin; notably, the weak hydrogen bond formed via Gln96 of the HLA molecule contributes to this behavior. We also clarified that these HLA molecules are easily accumulated in the endoplasmic reticulum, exhibiting a low expression on the cell surface. Considering that these hypersensitivity risk-associated HLA molecules form complexes with β_2-microglobulin and peptides in the endoplasmic reticulum, we assumed that their low complex formation ability in the endoplasmic reticulum facilitates the interaction with multiple drugs.

1. Introduction

Delayed drug hypersensitivity often leads to the development of fatal pathological conditions, such as Stevens–Jonson syndrome (SJS), toxic epidermal necrosis (TEN), drug-induced liver injuries (Daly et al., 2009), and drug reaction with eosinophilia and systemic symptoms (Taurog et al., 2009). Recent genome-wide association and cohort studies revealed that human leukocyte antigen (HLA) is associated with the development of drug hypersensitivity (Pan et al., 2017; Saag et al., 2008). Such examples include hypersensitivity due to HLA-B*57:01 and abacavir (Saag et al., 2008), SJS/TEN due to HLA-B*15:02 and carbamazepine (Chung et al., 2004), and SJS/TEN due to HLA-B*58:01 and allopurinol (Génin et al., 2011). Several other HLA polymorphisms have also been suggested to pose a risk of drug hypersensitivity (Ghattaoraya et al., 2016). In contrast, no association with drug hypersensitivity has been suggested for HLA-B*57:03 (belonging to a group of broad antigen serotype B17 and split antigen serotype B57, which differs by only two and five amino acids from that of HLA-B*57:01 and HLA-B*58:01, respectively), which have the same broad antigen serotype as that of HLA-B*57:01 (split antigen serotype B57) and HLA-B*58:01 (split antigen serotype B58). Similar behavior is seen with HLA-B*15:01 (belonging to a group of broad antigen serotype B15 and split antigen serotype B62, which differs by five amino acids from that of HLA-B*15:02) and with HLA-B*15:02 (split antigen serotype B75), suggesting that occurrence of drug hypersensitivity might depend on a specific HLA polymorphism. The association between HLA polymorphisms and the development of drug hypersensitivity has also been shown in recent HLA-introduced mouse models (Cardone et al., 2018; Susukida et al., 2018; Susukida et al., 2021), where it was suggested that an HLA polymorphism-specific immune response was elicited upon exposure to specific drugs.

Interestingly, HLA-B*57:01 is a risk factor for drug hypersensitivity not only upon exposure to abacavir but also to flucloxacillin and allopurinol (Daly et al., 2009; Mockenhaupt et al., 2019), while HLA-

* Corresponding author.
E-mail address: aokishigeki@chiba-u.jp (S. Aoki).

https://doi.org/10.1016/j.tiv.2022.105383
Received 22 March 2022; Received in revised form 4 May 2022; Accepted 9 May 2022
Available online 11 May 2022

B*15:02 has been linked to reactions occurring due to exposure to oxcarbazepine, lamotrigine, and sulfamethoxazole (Hu et al., 2011; Hung et al., 2010; Kongpan et al., 2015) and HLA-B*58:01 associated hypersensitivity due to carbamazepine and nevirapine (He et al., 2013; Phillips et al., 2013). This confirms that specific HLA polymorphisms are correlated with hypersensitivity reactions upon exposure to multiple drugs. However, the reason for certain HLA molecules behaving as risk factors for developing hypersensitivity reactions in response to multiple drugs remains unclear.

Several hypotheses have been proposed as the pathogenic mechanisms of HLA-dependent drug hypersensitivity. The following three hypotheses are representative (Yun et al., 2016): the hapten hypothesis suggests that a drug covalently binds to an antigenic peptide which is then presented by the HLA complex. The pharmacological interaction with an immune receptor (p-i) hypothesis recommends that the drug noncovalently binds to an HLA complex or T-cell receptor. Moreover, the altered peptide repertoire hypothesis reports that the drug alters the peptide repertoire. Under these hypotheses, specific drugs are anticipated to modify the HLA complex, thus creating immunogenicity and activating T-cells that recognize HLA. Considering the well-studied association between HLA-B*57:01 and hypersensitivity to abacavir exposure as an example, it was shown that the binding of abacavir to the peptide-binding groove of HLA-B*57:01 changes the repertoire of antigenic peptides, suggesting that HLA-B*57:01 carries a unique antigenic peptide that stimulates T-cells (Adam et al., 2014; Illing et al., 2012; Ostrov et al., 2012). Meanwhile, HLA-B*57:01 has also been associated with drug hypersensitivity due to multiple drug exposure, including abacavir. Therefore, implying that HLA molecules, including HLA-B*57:01, which pose a risk for developing drug hypersensitivity, have structural properties that facilitate interaction with multiple drugs.

HLA molecules are broadly classified into class I and class II. In general, class I molecules with A, B, and C antigen types form complexes with β_2-microglobulin (β_2m) and antigen peptides in the endoplasmic reticulum (ER) and are transported to the cell surface (Blum et al., 2013). However, when cells expressing HLA-B*57:01 were exposed to abacavir, it was found that they exhibited a cell surface presentation different from that of the classical one (i.e., HLA heavy chain alone or a dimer of HLA heavy chain and β_2m) (Shirayanagi et al., 2020). Hence, the structural characteristics of HLA molecules and the peculiar assembly of HLA complexes in the ER might be the reason for such nonclassical cell surface presentation.

In this study, considering the possibility that HLA molecules posing a risk for drug hypersensitivity might have structural characteristics different from that of non-risk HLA, we focused on the formation processes of HLA complexes based on HLA molecules and β_2m.

2. Materials and methods

2.1. Reagents

The following reagents were used in this study: anti-FLAG® M2 monoclonal antibody (Sigma-Aldrich, St Louis, MO, USA), anti-β_2m polyclonal antibody (GENETEX, Irvine, CA, USA), anti-GAPDH monoclonal antibody (Cell Signaling Technology, Beverly, MA, USA), anti-calnexin antibody (Abcam, Cambridge, UK), horseradish peroxidase-labeled anti-mouse IgG antibody (GE Healthcare, Chicago, IL, USA), horseradish peroxidase-labeled anti-rabbit IgG antibody (GE Healthcare), anti-mouse IgG Alexa® Fluor 488 (Abcam), anti-rabbit IgG Alexa® Fluor 546 (Thermo Fisher Scientific, Waltham, MA, USA), TO-PRO®-3 (Thermo Fisher Scientific), anti-FLAG® M2 magnetic beads (Sigma-Aldrich), EZ-Link™ NHS-Biotin (Thermo Fisher Scientific), and Pierce™ streptavidin magnetic beads (Thermo Fisher Scientific).

2.2. Cell culture

HeLa cells, purchased from RIKEN Cell Bank (Tsukuba, Japan), were maintained in a minimum essential medium (Nacalai Tesque, Kyoto, Japan) supplemented with 10% fetal bovine serum (Biosera, Nuaillé, France) plus antibiotic-antimycotic mixed solution (Nacalai Tesque) and nonessential amino acids solution (Nacalai Tesque). Cells were cultured at 37 °C in a humidified atmosphere of 5% CO_2 in the air.

2.3. Construction of an HLA expression vector

The HLA-B*57:01 expression vector (pcDNA-HLA-B*57:01) was constructed in our laboratory (Susukida et al., 2018). In short, HLA-B*57:01 cDNA was inserted into the pcDNA3.1D vector (Life Technologies, Grand Island, NY, USA) with 3× FLAG tags at the end of the C-terminus. HLA-B*57:03, HLA-B*15:01 (pcDNA-HLA-B*15:01), and HLA-B*15:02 expression vectors were constructed by modifying the pcDNA-HLA-B*57:01 (Shirayanagi et al., 2020). The HLA-B*15:11 expression vector was generated by site-directed mutagenesis of the pcDNA-HLA-B*15:01 (259G → A, 261G → C, and 272C → A). Their amino acid sequence alignments of the polymorphic antigen-presenting site are summarized in Supplementary Fig. 1. The HLA-B*57:03-Gln96Leu and the HLA-B*15:01-Gln96Leu expression vectors were generated by site-directed mutagenesis of the pcDNA-HLA-B*57:03 and B*15:01 (362A → T). The HLA-B*58:01 expression vector was constructed as follows: artificial cDNA of the HLA-B*58:01 extracellular region (purchased from Integrated DNA Technologies, Coralville, IA, USA) was replaced with the HLA-B*57:01 extracellular region sequence in pcDNA-HLA-B*57:01 using the In-Fusion® HD cloning kit (Takara bio, Kusatsu, Japan).

2.4. Introduction of HLA expression vector

HeLa cells were plated in flat-bottomed 12-well plates (1.0×10^5 cells/well). After 24 h, cells were transfected with the HLA expression vector using the Lipofectamine® 2000 reagent (Thermo Fisher Scientific) according to the manufacturer's instructions. After transfection for 24 h, cells were cultured with fresh medium for another 24 h.

2.5. Immobilization of HLA on anti-FLAG magnetic beads

HeLa cells expressing introduced HLA were lysed on ice in a lysis buffer containing 0.5% Nonidet P-40, 150 mM NaCl, 50 mM Tris-HCl (pH 8.0), and a protease inhibitor cocktail (Roche Diagnostic, Indianapolis, IN, USA). The concentration of protein in the lysis buffer was measured using a BCA™ protein assay kit (Thermo Fisher Scientific), according to the manufacturer's instructions. Then, 100 μg protein in 500 μL lysis buffer was incubated with 10 μL anti-FLAG® M2 magnetic beads overnight at 4 °C with gentle agitation. After washing the beads with lysis buffer, bound proteins were eluted with 100 μL 0.1 M glycine-HCl (pH 3.0) and neutralized with 20 μL solution containing 0.5 M Tris-HCl (pH 8.0) and 1.5 M NaCl.

2.6. Cell surface protein immobilization on streptavidin magnetic beads

HeLa cells expressing introduced HLA were biotinylated with 350 μL solution of 750 μg/mL EZ-Link™ NHS-Biotin in borate buffer (pH 9.0) containing 150 mM NaCl, 4 mM KCl, 1 mM $CaCl_2$, 0.5 mM $Mg_2Cl_2{\cdot}6H_2O$, 0.2 mM $MgSO_4{\cdot}7H_2O$, and 10 mM boric acid for 30 min at 4 °C. Biotinylated cells were lysed on ice as above. Then, 150 μg protein in 500 μL lysis buffer was incubated with 50 μL Pierce™ streptavidin magnetic beads for 4 h at 4 °C with gentle agitation. After incubation, magnetic beads were washed on ice with lysis buffer. Then, proteins were eluted by boiling the magnetic beads in sodium dodecyl sulfate-polyacrylamide gel electrophoresis (SDS-PAGE), reducing sample buffer containing 62.5 μM Tris-HCl (pH 6.8), 12.6% glycerol, 2% β-mercaptoethanol, 2% SDS, and bromophenol blue.

2.7. Immunoblotting

For immunoblotting, 10 μg protein in lysis buffer, 10 μL precipitated samples with anti-FLAG® M2 magnetic beads, or biotinylated samples were subjected to electrophoresis in a polyacrylamide gel containing 0.1% SDS. Separated proteins were then transferred to polyvinylidene difluoride (PVDF) membranes (Merck Millipore, Berlin, Germany). After blocking membranes with 5% bovine serum albumin (Nacalai Tesque) at 25 °C for 1 h, blots were incubated overnight at 4 °C with primary antibodies at a 1:1000 dilution. The membranes were then incubated for 1 h at 25 °C with the corresponding horseradish peroxidase-labeled secondary antibodies at a 1:5000 dilution. Bound antibodies were detected using the ECL prime detection reagent (GE Healthcare) and a LAS-4000 luminescent image analyzer (GE Healthcare). Images of the full-size membrane are available in Supplementary Fig. 2.

2.8. Immunofluorescence imaging

HeLa cells expressing introduced HLA were fixed in 4% paraformaldehyde (Nacalai Tesque) for 10 min at 4 °C and permeabilized in PBS containing 0.05% Triton X-100 for 10 min at 4 °C. After blocking cells with 1% bovine serum albumin at 25 °C for 30 min, cells were stained with anti-FLAG® M2 monoclonal antibody and anti-calnexin monoclonal antibody at a 1:200 dilution for 30 min at 25 °C. Secondary antibodies were added at a 1:200 dilution for 30 min at 25 °C. Nuclei were stained with TO-PRO®-3 stain (Thermo Fisher Scientific) for 5 min at 25 °C. Then, cells were mounted in Vectashield antifade mounting medium (Vector Laboratories, Burlingame, CA, USA). Immunofluorescence images were captured under a Zeiss LSM 700 confocal microscope equipped with Airyscan and ZEN software (Zeiss, Jena, Germany).

2.9. Molecular Dynamics (MD) simulation

MD simulations were performed using the AMBER16 package, as previously described (Jaruthamsophon et al., 2017). The crystal structures of the heterotrimeric complexes of the extracellular domain of HLA heavy chain, β_2m and antigen peptide were downloaded from the protein data bank (PDB). After removing the antigen peptide, the HLA-β_2m heterodimer of HLA-B*57:01, HLA-B*57:03, HLA-B*58:01, HLA-B*15:01, and HLA-B*15:02 (PDB ID code 5VUF, 5VWF, 5VWH, 6VB3, and 6VB4, respectively (Illing et al., 2018)), served as starting structures for MD simulations. All heterodimer complexes were solvated with TIP3P (transferable intermolecular potential 3P) water in an octahedron box maintaining a buffering distance of 10 Å between the complex surface and box boundary. Counter ions were added to neutralize each model system using the LEaP module of AMBER16. All prepared systems were minimized in two steps. Water molecules and ions were initially minimized by keeping force restraints over the complexes, followed by minimization of the whole system in the second setup. The first 3000 steps of energy minimization were run using the steepest descent method, whereas the remaining 7000 steps were run using the conjugate gradient method. After minimization, each system was gently allowed to heat from 0 to 310 K at 100 ps at constant volume and equilibrated at 310 K for another 400 ps at constant pressure. Finally, a production run was performed with no restraints imposed for 200 ns in an isothermal isobaric (NPT) ensemble, and a time step of 2 fs was adopted.

2.10. Trajectory analysis

The calculations of the root mean square deviation (RMSD) and root mean square fluctuation (RMSF) were performed using CPPTRAJ (Roe and Cheatham, 2013). The calculation of the migration distance of each atom and the Student's *t*-test were performed using Microsoft Excel (Redmond, WA, USA).

3. Results

3.1. HLA-B risk molecules associated with drug hypersensitivity had a lower affinity for β_2m than non-risk variants

A newly synthesized HLA heavy chain forms a heterodimer with subunit β_2m, followed by the loading of the heterodimer with an antigenic peptide before being expressed on the cell surface. Accordingly, the affinity between the HLA heavy chain and β_2m can be a parameter that greatly influences the efficiency of HLA complex formation and surface expression. To evaluate the strength of affinity of the HLA heavy with β_2m, we compared the concentration of β_2m bound to the HLA heavy chain between risk and non-risk HLA molecules. We introduced 3 × FLAG-tagged HLA heavy chain and β_2m into HeLa cells and then immunoprecipitated the HLA from cell lysates using an anti-FLAG® M2 monoclonal antibody. We found that the amount of β_2m immunoprecipitated with HLA-B*57:01 and HLA-B*58:01 (both risks) was lower than that with HLA-B*57:03 (non-risk). Likewise, the amount of β_2m immunoprecipitated with HLA-B*15:02 and HLA-B*15:11 (both risks, HLA-B*15:11 belongs to the group of broad antigen serotype B15 and split antigen serotype B75) was lower than that with HLA-B*15:01 (non-risk) (Fig. 1). In addition, we found that risk molecules showed a slightly lower amount of HLA heavy chain present in the whole cell lysate compared with that in the non-risk molecule (Fig. 1). These results suggested that risk HLA molecules have lower affinity for β_2m than non-risk, which might influence the HLA expression and complex formation.

3.2. Flexibility of residues that form hydrogen bonds between the HLA heavy chain and β_2m

We found that the risk HLA heavy chains had a low affinity for β_2m (Fig. 1). To investigate the cause of this weak interaction, we performed MD simulations to evaluate the flexibility of the HLA-β_2m heterodimer complex. We initially focused on the HLA complex (HLA heavy chain

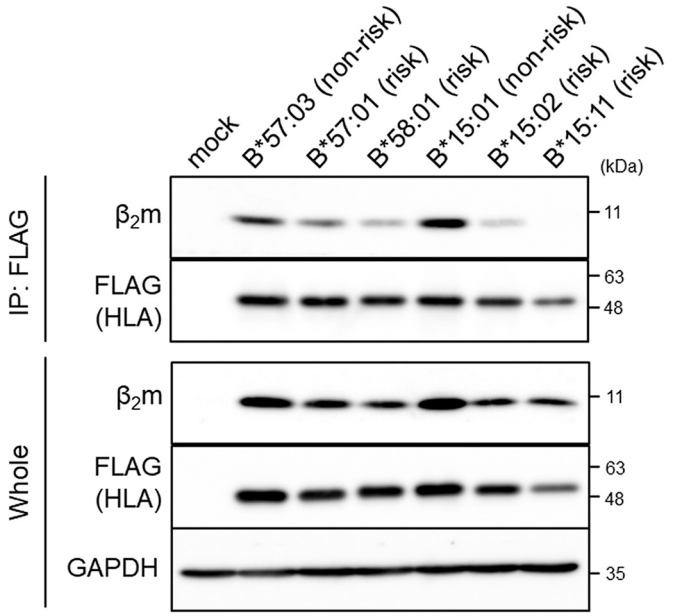

Fig. 1. HLA-B risk molecules associated with drug hypersensitivity have a lower affinity with β_2m than non-risk variants. Lysates of HLA-introduced HeLa cells were subjected to immunoprecipitation using anti-FLAG® M2 monoclonal antibody magnetic beads. FLAG-tagged protein (equivalent to HLA heavy chain protein) and β_2m were detected by western blotting (IP: FLAG). Each whole cell lysate sample was also subjected to western blot analysis to detect the FLAG-tagged protein and β_2m (Whole). GAPDH protein was used as the loading control.

and β_2m) and evaluated the RMSD of the atoms that constitute each main chain (Fig. 2a). However, we did not observe any clear difference between risk and non-risk HLAs, the RMSD of which remained stable at approximately 1.0–2.0 Å for the entire calculated time of 100 ns. Next, we calculated the RMSF of each residue at the end of the 100 ns because all complexes were stable during this period (Fig. 2b). Accordingly, we found that risk HLAs showed higher RMSF values in some residues than non-risk HLAs. Especially, the RMSF value of Gln96 in HLA-B*57:01 (0.5452 Å) and HLA-B*58:01 (0.7312 Å) was higher than that in HLA-B*57:03 (0.5214 Å). To determine whether there was a significant difference in oscillation between risk and non-risk HLAs, we calculated whether there was a remarkable difference in the migration distance per ns for each atom of the residues associated with hydrogen bonding (Tysoe-Calnon et al., 1991). As a result, we detected that risk HLAs oscillated more violently than non-risk HLAs at Gln96 and Asp122, in both HLA-B17 (Table 1) and HLA-B15 (Table 2) serotypes. These two residues constitute hydrogen bonds with β_2m in the F pocket at the HLA peptide-binding groove.

3.3. *HLA alleles associated with drug hypersensitivity accumulated in the ER*

Our in vitro and in silico data suggested that risk HLAs (HLA-B*57:01, HLA-B*58:01, HLA-B*15:02, and HLA-B*15:11) were less likely to have a weak affinity for β_2m. Therefore, we assumed that risk HLAs might accumulate in the ER, where they are synthesized. We next evaluated the subcellular localization of HLA and assessed whether this weak affinity between HLA and β_2m affects the localization of HLA molecules. We observed that most HLA-B*57:03 did not overlap with calnexin, an ER-marker, whereas a large part of HLA-B*57:01 and B*58:01 overlapped with calnexin (Fig. 3a), suggesting a tendency for retention of these risk HLAs in the ER. To confirm that their accumulation in the ER was due to the weak affinity between the HLA heavy chain and β_2m, we introduced a Gln96Leu mutant of HLA, which cannot bind to β_2m via hydrogen bonds (Tysoe-Calnon et al., 1991). Our MD simulations also indicated that the flexibility of Gln96 affected the HLA-β_2m binding. Accordingly, we found that most HLA-B*57:03-Gln96Leu, which had an extremely weak affinity to β_2m (Fig. 3b), overlapped with calnexin (Fig. 3a), supporting our hypothesis. We also confirmed that risk HLAs were likely to accumulate in the ER using HLA-B15 serotypes (Fig. 3a, b). In addition, we examined the cell surface expression of HLAs using cell surface biotinylation assays. We observed that risk HLAs and HLA-Gln96Leu mutants showed lower levels of expression than non-risk HLAs (Fig. 3c), implying that risk HLAs were accumulated in the ER. Conclusively, we assumed that the high accumulation of risk HLAs in the ER and their relatively lower expression on the cell surface might be due to the weak affinity between the HLA heavy chain and β_2m.

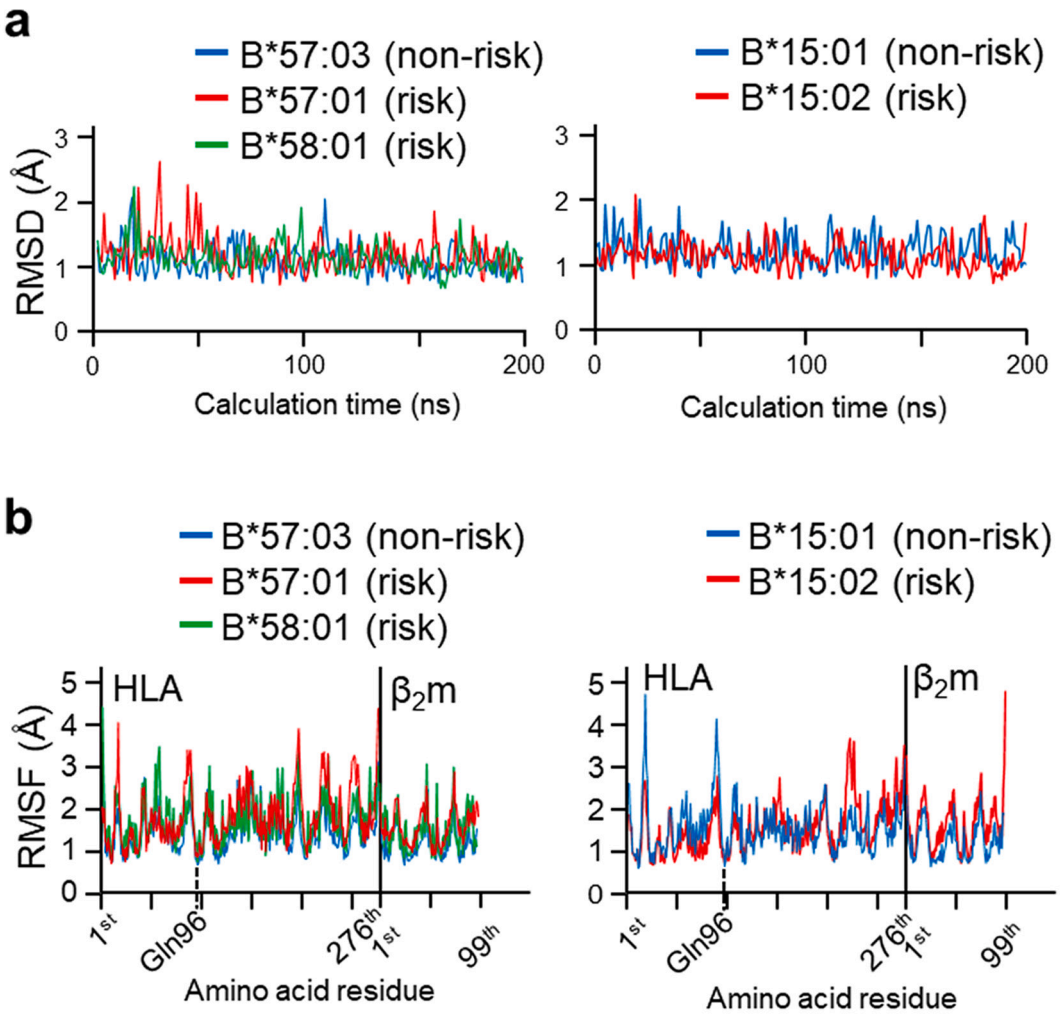

Fig. 2. Flexibility of residues that form hydrogen bonds between the HLA heavy chain and β_2m. (a) Root mean square deviation (RMSD) vs. time plot of whole main chain atoms of each HLA-β_2m complex, HLA-B*57:03 (left blue), HLA-B*57:01 (left red), HLA-B*58:01 (left green), HLA-B*15:01 (right blue), and HLA-B*15:02 (right red). (b) RMSF vs. residue of each HLA-β_2m complex, HLA-B*57:03 (left blue), HLA-B*57:01 (left red), HLA-B*58:01 (left green), HLA-B*15:01 (right blue), and HLA-B*15:02 (right red). (For interpretation of the references to colour in this figure legend, the reader is referred to the web version of this article.)

Table 1
Migration distance of each atom in HLA-B*57:01 (risk), B*57:03 (non-risk), and B*58:01 (risk) residues that relate to HLA-β_2m hydrogen bonds. Bold values are significantly larger than those in the control allele HLA-B*57:03 ($p < 0.05$).

Residue	Atom	Mean migration distance ± S.D.		
		B*57:03 (PDB:5VWF)	B*57:01 (PDB:5VUF)	B*58:01 (PDB:5VWH)
Tyr27 (D pocket)	N	0.653 ± 0.291	0.622 ± 0.269	0.647 ± 0.268
	C_A	0.667 ± 0.295	0.654 ± 0.297	0.653 ± 0.266
	C_B	0.747 ± 0.333	0.779 ± 0.373	0.752 ± 0.318
	C_G	0.792 ± 0.349	0.776 ± 0.400	0.744 ± 0.309
	C_{D1}	0.951 ± 0.452	0.953 ± 0.525	0.839 ± 0.410
	C_{E1}	1.076 ± 0.519	1.037 ± 0.584	0.884 ± 0.441
	C_Z	1.074 ± 0.517	0.992 ± 0.495	0.872 ± 0.412
	O_H	1.279 ± 0.646	1.157 ± 0.560	1.027 ± 0.497
	C_{E2}	1.067 ± 0.534	1.051 ± 0.577	0.933 ± 0.455
	C_{D2}	0.938 ± 0.467	0.961 ± 0.548	0.866 ± 0.406
	Cα	0.680 ± 0.282	0.681 ± 0.307	0.652 ± 0.280
	O	0.810 ± 0.339	0.723 ± 0.311	0.719 ± 0.305
Gln32 (A pocket)	N	0.851 ± 0.411	0.800 ± 0.363	0.785 ± 0.319
	C_A	0.808 ± 0.373	0.738 ± 0.328	0.756 ± 0.322
	C_B	0.885 ± 0.411	0.800 ± 0.376	0.872 ± 0.375
	C_G	0.912 ± 0.436	0.803 ± 0.379	0.993 ± 0.573
	C_D	0.787 ± 0.361	0.796 ± 0.362	0.950 ± 0.532
	O_{E1}	1.179 ± 0.609	0.992 ± 0.529	1.129 ± 0.679
	N_{E2}	0.878 ± 0.480	0.810 ± 0.405	1.177 ± 0.767
	Cα	0.820 ± 0.385	0.733 ± 0.309	0.777 ± 0.345
	O	0.976 ± 0.461	0.852 ± 0.381	0.932 ± 0.437
Arg35 (A pocket)	N	0.665 ± 0.290	0.622 ± 0.300	0.616 ± 0.315
	C_A	0.658 ± 0.268	0.632 ± 0.314	0.622 ± 0.308
	C_B	0.739 ± 0.311	0.667 ± 0.343	0.686 ± 0.345
	C_G	0.877 ± 0.481	0.761 ± 0.425	0.857 ± 0.509
	C_D	1.118 ± 0.637	0.861 ± 0.481	1.027 ± 0.578
	N_E	1.359 ± 0.826	0.845 ± 0.498	1.169 ± 0.536
	C_Z	1.790 ± 1.197	1.009 ± 0.682	1.318 ± 0.677
	N_{H1}	2.243 ± 1.467	1.287 ± 0.934	1.445 ± 0.781
	N_{H2}	2.124 ± 1.580	1.120 ± 0.818	1.621 ± 0.999
	Cα	0.651 ± 0.278	0.634 ± 0.304	0.629 ± 0.318
	O	0.718 ± 0.304	0.676 ± 0.318	0.687 ± 0.344
Arg48 (A pocket)	N	0.883 ± 0.394	0.896 ± 0.400	0.812 ± 0.378
	C_A	0.942 ± 0.450	0.961 ± 0.458	0.878 ± 0.413
	C_B	1.006 ± 0.486	0.986 ± 0.491	0.922 ± 0.424
	C_G	1.171 ± 0.631	1.241 ± 0.714	1.053 ± 0.726
	C_D	1.424 ± 0.835	1.278 ± 0.718	1.134 ± 0.806
	N_E	1.388 ± 0.779	1.146 ± 0.651	1.024 ± 0.547
	C_Z	1.675 ± 0.965	1.325 ± 0.769	1.174 ± 0.714
	N_{H1}	2.029 ± 1.228	1.687 ± 0.959	1.451 ± 0.965
	N_{H2}	1.846 ± 1.142	1.423 ± 0.933	1.283 ± 0.738
	Cα	1.099 ± 0.570	1.035 ± 0.507	0.991 ± 0.464
	O	1.396 ± 0.802	1.423 ± 0.752	1.285 ± 0.667
Gln96 (F pocket)	N	0.535 ± 0.217	0.586 ± 0.292	0.574 ± 0.262
	C_A	0.504 ± 0.204	0.563 ± 0.276	0.559 ± 0.249
	C_B	0.549 ± 0.223	**0.633 ± 0.288**	**0.622 ± 0.286**
	C_G	0.625 ± 0.255	0.658 ± 0.292	0.691 ± 0.314
	C_D	0.644 ± 0.225	0.682 ± 0.311	0.681 ± 0.314
	O_{E1}	0.723 ± 0.287	**0.845 ± 0.392**	0.809 ± 0.369
	N_{E2}	0.731 ± 0.279	0.765 ± 0.317	0.756 ± 0.378
	Cα	0.490 ± 0.199	**0.574 ± 0.315**	**0.568 ± 0.276**
	O	0.553 ± 0.242	0.641 ± 0.374	**0.664 ± 0.342**
Asp122 (F pocket)	N	0.821 ± 0.322	**0.926 ± 0.397**	**0.941 ± 0.391**
	C_A	0.807 ± 0.316	0.896 ± 0.407	0.902 ± 0.390
	C_B	0.991 ± 0.426	1.045 ± 0.480	1.098 ± 0.485
	C_G	1.180 ± 0.547	**1.369 ± 0.629**	**1.359 ± 0.621**
	O_{D1}	1.988 ± 0.854	2.088 ± 1.000	2.052 ± 0.968
	O_{D2}	1.900 ± 0.903	2.129 ± 0.938	2.042 ± 1.013
	Cα	0.772 ± 0.330	0.858 ± 0.410	0.860 ± 0.406
	O	0.845 ± 0.361	**1.003 ± 0.469**	**0.971 ± 0.480**

Table 2
Migration distance of each atom in HLA-B*15:01 (non-risk) and B*15:02 (risk) residues that relate to HLA-β_2m hydrogen bonds. Bold values are significantly larger than those in the control allele HLA-B*15:01 ($p < 0.05$).

Residue	Atom	Mean migration distance ± S.D.	
		B*15:01(PDB:6VB3)	B*15:02(PDB:6VB4)
Tyr27 (D pocket)	N	0.503 ± 0.234	**0.580 ± 0.252**
	C_A	0.519 ± 0.252	0.590 ± 0.257
	C_B	0.618 ± 0.278	0.656 ± 0.263
	C_G	0.620 ± 0.262	0.669 ± 0.324
	C_{D1}	0.792 ± 0.418	0.837 ± 0.523
	C_{E1}	0.888 ± 0.440	0.908 ± 0.684
	C_Z	0.830 ± 0.335	0.878 ± 0.679
	O_H	0.986 ± 0.465	1.068 ± 0.866
	C_{E2}	0.801 ± 0.369	0.894 ± 0.615
	C_{D2}	0.702 ± 0.339	0.792 ± 0.441
	Cα	0.522 ± 0.239	0.586 ± 0.287
	O	0.586 ± 0.259	0.653 ± 0.323
Gln32 (A pocket)	N	0.642 ± 0.266	**0.755 ± 0.386**
	C_A	0.575 ± 0.244	**0.682 ± 0.353**
	C_B	0.616 ± 0.276	**0.743 ± 0.388**
	C_G	0.641 ± 0.292	**0.798 ± 0.446**
	C_D	0.614 ± 0.281	**0.943 ± 0.614**
	O_{E1}	0.911 ± 0.573	1.045 ± 0.728
	N_{E2}	0.673 ± 0.359	**1.239 ± 1.115**
	Cα	0.570 ± 0.272	**0.683 ± 0.379**
	O	0.678 ± 0.335	**0.816 ± 0.433**
Arg35 (A pocket)	N	0.525 ± 0.256	**0.616 ± 0.285**
	C_A	0.537 ± 0.250	0.603 ± 0.272
	C_B	0.634 ± 0.291	0.654 ± 0.311
	C_G	0.795 ± 0.365	0.786 ± 0.341
	C_D	1.051 ± 0.625	0.926 ± 0.487
	N_E	1.258 ± 0.805	1.081 ± 0.694
	C_Z	1.708 ± 1.174	1.324 ± 0.861
	N_{H1}	2.103 ± 1.450	1.555 ± 0.951
	N_{H2}	2.012 ± 1.547	1.611 ± 1.188
	Cα	0.551 ± 0.248	0.608 ± 0.283
	O	0.629 ± 0.267	0.680 ± 0.308
Arg48 (A pocket)	N	0.751 ± 0.369	0.773 ± 0.353
	C_A	0.779 ± 0.365	0.835 ± 0.393
	C_B	0.866 ± 0.500	0.922 ± 0.505
	C_G	1.051 ± 0.596	1.095 ± 0.607
	C_D	0.990 ± 0.555	0.977 ± 0.573
	N_E	1.239 ± 0.660	1.129 ± 0.779
	C_Z	1.509 ± 0.840	1.373 ± 0.828
	N_{H1}	1.343 ± 0.782	1.298 ± 1.036
	N_{H2}	0.835 ± 0.416	0.792 ± 0.353
	Cα	1.141 ± 0.662	0.937 ± 0.465
	O	0.796 ± 0.378	0.868 ± 0.427
Gln96 (F pocket)	N	0.507 ± 0.207	0.565 ± 0.275
	C_A	0.483 ± 0.190	0.531 ± 0.253
	C_B	0.524 ± 0.207	0.588 ± 0.261
	C_G	0.526 ± 0.223	**0.719 ± 0.341**
	C_D	0.557 ± 0.239	**0.683 ± 0.293**
	O_{E1}	0.687 ± 0.277	**0.787 ± 0.379**
	N_{E2}	0.635 ± 0.285	**0.768 ± 0.307**
	Cα	0.502 ± 0.213	0.513 ± 0.276
	O	0.561 ± 0.264	0.615 ± 0.345
Asp122 (F pocket)	N	0.818 ± 0.362	0.886 ± 0.360
	C_A	0.767 ± 0.332	**0.887 ± 0.370**
	C_B	0.922 ± 0.429	**1.106 ± 0.480**
	C_G	1.185 ± 0.603	1.327 ± 0.673
	O_{D1}	2.181 ± 0.929	2.187 ± 0.885
	O_{D2}	1.915 ± 0.912	2.000 ± 0.945
	Cα	0.723 ± 0.311	0.799 ± 0.359
	O	0.850 ± 0.402	0.917 ± 0.405

3.4. HLA molecules associated with drug hypersensitivity had a lower affinity for tapasin

These risk HLAs tended to accumulate in the ER possibly due to their low affinity for β_2m. In general, newly synthesized HLA forms a heterodimer with β_2m in the ER, followed by the binding of the heterodimer to several proteins, including tapasin, forming a peptide-loading complex (PLC) to load an antigen peptide (Blum et al., 2013). After loading the antigen peptide, the HLA heterotrimeric complex dissociates from the PLC and escapes the ER to the cell surface. However, the risk HLAs forming these complexes slower is indicated to have difficulty in dissociating from PLC. Therefore, we evaluated the binding of HLAs to tapasin to compare the amount of HLA integrated into the PLC. We found that the risk HLAs (HLA-B*57:01, HLA-B*58:01, and HLA-B*15:02) bind to tapasin more strongly than the non-risk HLAs (HLA-

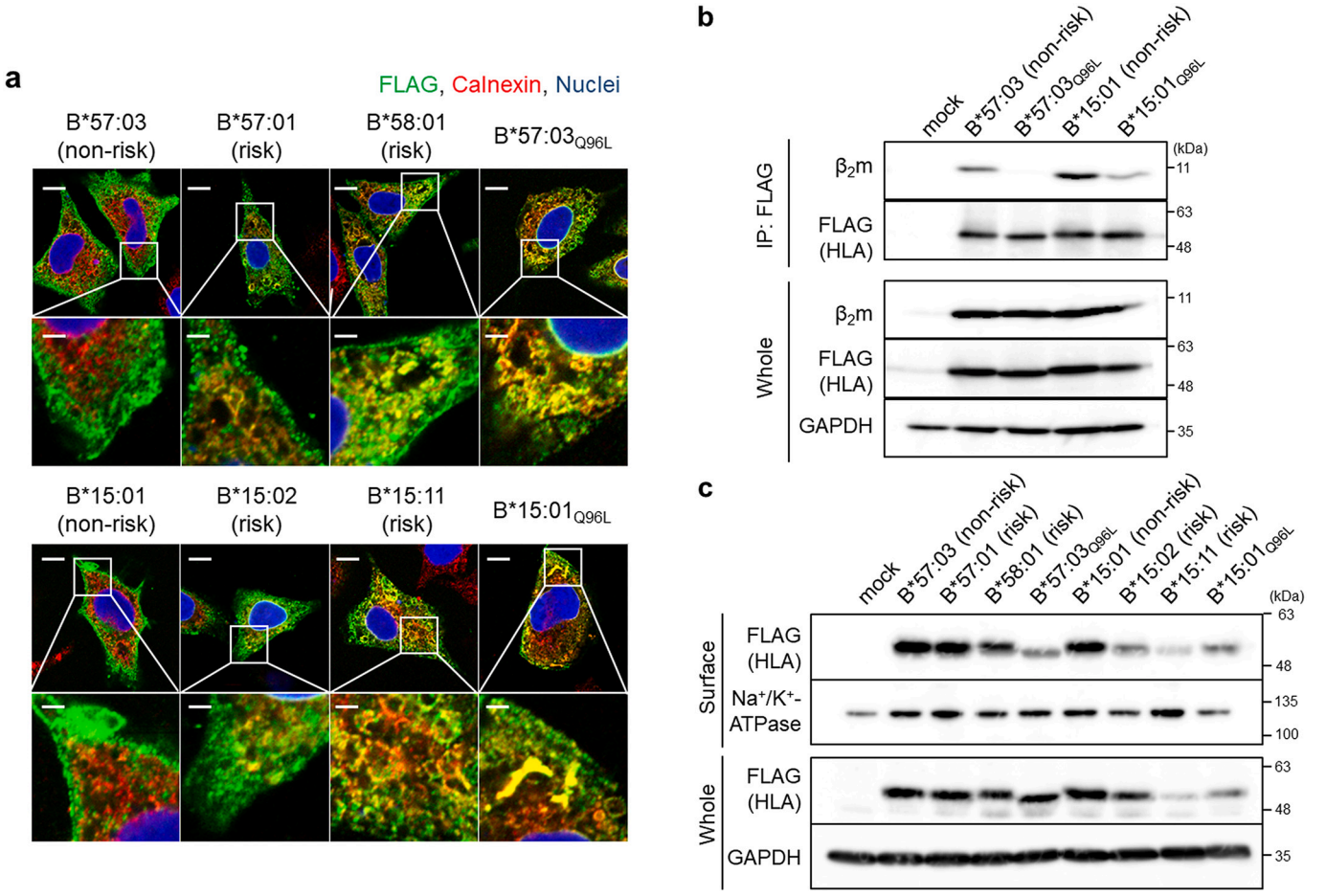

Fig. 3. HLA alleles associated with drug hypersensitivity accumulate in the endoplasmic reticulum. (a) HLA-introduced HeLa cells were stained using anti-FLAG® M2 monoclonal (green) and anti-calnexin (red) antibodies. Nuclei were stained using TO-PRO®-3 (blue). Scale bars represent 10 μm (upper) and 2.5 μm (lower, enlarged). (b) Lysates of HLA-introduced HeLa cells were subjected to immunoprecipitation using anti-FLAG® M2 monoclonal antibody magnetic beads. FLAG-tagged protein (equivalent to HLA protein) and β_2m were detected by western blotting (IP: FLAG). Each whole cell lysate sample was subjected to western blot analysis to detect the FLAG-tagged protein and β_2m (Whole). GAPDH protein was used as the loading control. (c) Surface proteins of HLA-introduced HeLa cells were biotinylated and precipitated using streptavidin magnetic beads. FLAG-tagged protein (equivalent to HLA protein) was detected by western blot analysis (Surface). Whole cell lysates were subjected to western blot analysis to detect the FLAG-tagged protein (Whole). Na^+/K^+ ATPase and GAPDH proteins were used as loading controls. (For interpretation of the references to colour in this figure legend, the reader is referred to the web version of this article.)

B*57:03, HLA-B*15:01) (Fig. 4). In addition, HLA-B*15:11 showed a lower affinity for tapasin than HLA-B*15:01, while the HLA-Gln96Leu mutants were rarely bound to tapasin (Fig. 4), implying that in order for HLA to bind to tapasin it should be able to bind to β_2m to some extent. Overall, the high affinity between the risk HLAs and tapasin indicated that these HLA risk molecules in the ER are highly integrated into the PLC, where HLAs have inefficient complex formation ability with β_2m and antigen peptide.

4. Discussion

Our study highlighted the importance of focusing on the affinity between heavy chains and β_2m and the accumulation of HLA molecules in the ER for understanding the drug hypersensitivity associated with HLA polymorphisms. Multiple HLA molecules pose a risk of developing hypersensitivity, including HLA-B*57:01, which are presumed to be unlikely to form a heterotrimeric complex with β_2m and antigen peptides (Shirayanagi et al., 2020). These molecules have been shown to have a lower affinity for β_2m compared with non-risk HLA polymorphisms. Perhaps due to this property, a substantial amount of HLA-B*57:01 is accumulated in the ER; however, Ostrov et al. suggested the possibility of the HLA-B*57:01 molecule binding to abacavir at the stage of the HLA complex formation in the ER, thus changing the antigenic peptide to be loaded (Ostrov et al., 2012). In addition, we found that while a normal HLA-B complex forms a heterotrimeric complex with β_2m and antigen peptides on the cell surface, some HLA-B*57:01 molecules expressed on the cell surface did not have the heterotrimer structure, and the ratio of such structures was increased after exposure to abacavir (Shirayanagi et al., 2020). From these results, we inferred that the binding of a drug such as abacavir to HLA-B*57:01 at the stage of complex formation in the ER leads to abnormalities in the structure at the time of surface expression. Additionally, the low assembly efficiency of the HLA-B*57:01 complex facilitates its accumulation in the ER, potentially promoting its binding to abacavir and other drugs and rendering abnormal the structure of HLA expressed on the cell surface thus resulting in increased risk for drug hypersensitivity.

The low assembly efficiency of the HLA-B*57:01 complex that facilitates its accumulation in the ER might make the intracellular environment prone to stress during the synthesis of HLA complexes, which might also facilitate the onset of drug hypersensitivity. Martin et al. found that, in peripheral blood mononuclear cells (PBMC) taken from patients with HLA-B*57:01 and abacavir-induced hypersensitivity, exposure to abacavir-induced the expression of HSP70, large amounts of which were localized in the ER and endosomes. Additionally, they found that exposure to abacavir led to colocalization of HLA-B*57:01 and HSP70, and the expression level of the inflammatory cytokine IFN-γ was

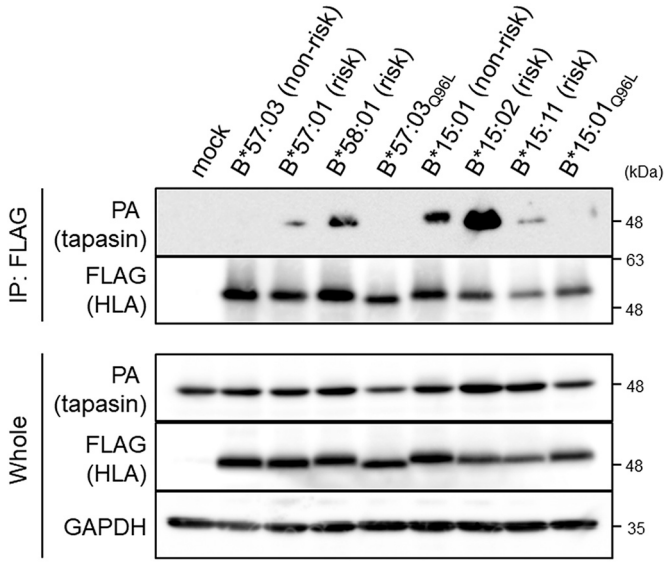

Fig. 4. HLA molecules associated with drug hypersensitivity have a lower affinity for tapasin. Lysates of HLA- and tapasin-introduced HeLa cells were subjected to immunoprecipitation using anti-FLAG® M2 monoclonal antibody magnetic beads. FLAG-tagged (equivalent to HLA protein) and PA-tagged (equivalent to tapasin) proteins were detected by western blot analysis (IP: FLAG). Each lysate sample was subjected to western blot analysis to detect the FLAG-tagged and PA-tagged proteins (Whole). GAPDH protein was used as the loading control.

correlated with the high expression level of HSP70 (Martin et al., 2007). Studies have suggested that HSP70 binds to misfolded proteins (Morishima, 2005), following its ER stress-induced expression (Brostrom and Brostrom, 1998), and mutations in HSP70 potentiate the risk for abacavir-induced hypersensitivity (Martin et al., 2004). Interpretation of these findings by Martin et al., along with the poor assembly property of HLA-B*57:01 and its tendency to accumulate in the ER, led us to infer the following scheme: (1) HLA accumulates in the ER due to poor complex assembly efficiency. (2) In the ER, HLA binds to abacavir and undergoes structural changes that result in a structure that is abnormal enough to bind HSP70. (3) This complex then induces ER stress, which leads to downstream immune activation such as cytokine induction. We observed surface expression of abnormally structured HLA in HLA-B*57:01-expressing cells when exposed to abacavir, which was not observed in HLA-B*57:03-expressing cells (Shirayanagi et al., 2020). This result supports the above schemes (1) and (2).

Martin et al. reported that individuals carrying both HLA-B*57:01 and mutant HSP70 do not necessarily elicit an immune response to abacavir (Martin et al., 2004). Therefore, there might be other causes behind the onset of drug hypersensitivity other than these two risk factors. Proteins that constitute PLC, such as tapasin, are also factors that aid in the assembly of HLA complexes and have been strongly associated with the accumulation of HLA molecules in the ER (Blum et al., 2013). Hence, the possibility of their involvement in the onset of drug hypersensitivity cannot be ruled out. As the affinity between tapasin and HLA risk molecules is high and previous studies indicated that the cell surface expression of HLA-B*57:01 was further decreased due to tapasin deficiency compared with that of HLA-B*57:03 (Rizvi et al., 2014), the accumulation of HLA in the ER and efficiency of PLC formation might be related to the onset of drug hypersensitivity. In addition, the level of expression and activity of proteins that constitute PLC, such as tapasin, is known to change depending on factors such as genotype and infection history (Perria et al., 2006; Wycisk et al., 2011), with the level of expression varying depending on the tissue (The Human Protein Atlas, https://www.proteinatlas.org/). In the lesion site of patients who develop drug hypersensitivity, the low level of PLC formation might cause a more profound accumulation of risk HLAs in the ER and facilitate the response to the drug. In summary, when explaining the individual differences and tissue specificity in the development of drug hypersensitivity, it is necessary to consider proteins that constitute PLC, such as tapasin, in addition to HLA polymorphisms.

In the present study, calculating the RMSD of entire HLA molecules associated with drug hypersensitivity and evaluating their flexibility revealed the lack of large differences between polymorphisms. However, the flexibility of HLA residues that form hydrogen bonds with β_2m was shown to be high in risk HLAs, which might indicate the risk of developing drug hypersensitivity. This result suggested the possibility of evaluating the risk of drug hypersensitivity posed by a HLA polymorphism by evaluating only the residues that form hydrogen bonds with β_2m. Autoimmune diseases for which involvement of HLA-B has been repeatedly reported include ankylosing spondylitis (HLA-B*27:05, B*27:04, and B*15:02 pose risk) (Loll et al., 2016; Wu et al., 2020), Behcet's disease (HLA-B*51:01, B*57, B*35, and B*27 pose risk) (Adeeb et al., 2017; Gul and Ohno, 2012), and psoriasis (HLA-B*57:01 and B*27 pose risk) (Hentzien et al., 2020; Queiro et al., 2016). In addition, risk HLA polymorphisms for drug hypersensitivity have often been reported to correlate with autoimmune diseases as well. Based on these results, we speculated that the evaluation of flexibility of the hydrogen bonding residues in the HLA heavy chain-β_2m might be useful for evaluating the risk of developing autoimmune diseases and drug hypersensitivity. In the past, MD simulations for evaluating the risk of autoimmune diseases posed by HLA polymorphism were conducted on HLA-B*27:05 (risk polymorphism) and HLA-B*27:09 (non-risk polymorphism). These simulations showed that the antigen-presenting site of the HLA was more flexible in risk HLAs of ankylosing spondylitis; the loaded antigenic peptide was also shown to be highly flexible (Abualrous et al., 2015). The weak affinity of the HLA-B27 polymorphism with β_2m has also been suggested to pose a risk for ankylosing spondylitis (Tsai et al., 2002), and the weak hydrogen bonding of the HLA heavy chain with β_2m might correlate with the flexibility of the antigen-presenting site and the high flexibility of the loaded peptide. Considering that the risk HLA polymorphisms for drug hypersensitivity investigated in this study had a high affinity to tapasin, the weak hydrogen bonding between the heavy chain of risk HLA polymorphisms and β_2m might contribute not only to the heterodimer structure of HLA-β_2m, but also the instability of the heterotrimeric structure of the HLA-β_2m-peptide that is associated with the flexibility of the antigen-presenting site.

Based on this study, it appears useful to evaluate the interaction of HLA-β_2m in preclinical development to predict and avoid drug hypersensitivity in patients. Predicting the onset of HLA polymorphism-dependent drug hypersensitivity has been considered practically difficult due to various HLA polymorphisms and the combination of compounds and drugs to be evaluated. In the future, it might become possible to predict the onset of toxicity more easily by evaluating the affinity between HLA molecules and β_2m to identify risk HLA polymorphisms and studying whether or not they invoke a response following drug exposure.

Declaration of Competing Interest

The authors declare that they have no known competing financial interests or personal relationships that could have appeared to influence the work reported in this paper.

Acknowledgments

This work was supported by Grant-in-Aid for Scientific Research (B) (21H02640 and 19H03386) from the Japan Society for the Promotion of Science and by JST SPRING (JPMJSP2109). The authors thank the Takeda Science Foundation. The authors would like to thank Editage (www.editage.com) for English language editing.

Appendix A. Supplementary data

Supplementary data to this article can be found online at https://doi.org/10.1016/j.tiv.2022.105383.

References

Abualrous, E.T., Fritzsche, S., Hein, Z., Al-Balushi, M.S., Reinink, P., Boyle, L.H., Wellbrock, U., Antoniou, A.N., Springer, S., 2015. F pocket flexibility influences the tapasin dependence of two differentially disease-associated MHC Class I proteins. Eur. J. Immunol. 45, 1248–1257.

Adam, J., Wuillemin, N., Watkins, S., Jamin, H., Eriksson, K.K., Villiger, P., Fontana, S., Pichler, W.J., Yerly, D., 2014. Abacavir induced T cell reactivity from drug Naïve individuals shares features of Allo-immune responses. PLoS One 9, e95339.

Adeeb, F., Ugwoke, A., Stack, A.G., Fraser, A.D., 2017. Associations of HLA-B alleles with Behçet's disease in Ireland. Clin. Exp. Rheumatol. 35 (Suppl. 104), 22–23.

Blum, J.S., Wearsch, P.A., Cresswell, P., 2013. Pathways of antigen processing. Annu. Rev. Immunol. 31, 443–473.

Brostrom, C.O., Brostrom, M.A., 1998. Regulation of translational initiation during cellular responses to stress. Prog. Nucleic Acid Res. Mol. Biol. 58, 79–125.

Cardone, M., Garcia, K., Tilahun, M.E., Boyd, L.F., Gebreyohannes, S., Yano, M., Roderiquez, G., Akue, A.D., Juengst, L., Mattson, E., Ananthula, S., Natarajan, K., Puig, M., Margulies, D.H., Norcross, M.A., 2018. A transgenic mouse model for HLA-B*57:01-linked abacavir drug tolerance and reactivity. J. Clin. Invest. 128, 2819–2832.

Chung, W.H., Hung, S.I., Hong, H.S., Hsih, M.S., Yang, L.C., Ho, H.C., Wu, J.Y., Chen, Y. T., 2004. Medical genetics: A marker for Stevens–Johnson syndrome. Nature. 428, 486.

Daly, A.K., Donaldson, P.T., Bhatnagar, P., Shen, Y., Pe'er, I., Floratos, A., Daly, M.J., Goldstein, D.B., John, S., Nelson, M.R., Graham, J., Park, B.K., Dillon, J.F., Bernal, W., Cordell, H.J., Pirmohamed, M., Aithal, G.P., Day, C.P., DILIGEN Study, International SAE Consortium, 2009. HLA-B*5701 genotype is a major determinant of drug-induced liver injury due to flucloxacillin. Nat. Genet. 41, 816–819.

Génin, E., Schumacher, M., Roujeau, J.C., Naldi, L., Liss, Y., Kazma, R., Sekula, P., Hovnanian, A., Mockenhaupt, M., 2011. Genome-wide association study of Stevens-Johnson syndrome and toxic epidermal necrolysis in Europe. Orphanet J. Rare Dis. 6, 52.

Ghattaoraya, G.S., Dundar, Y., González-Galarza, F.F., Maia, M.H., Santos, E.J., da Silva, A.L., McCabe, A., Middleton, D., Alfirevic, A., Dickson, R., Jones, A.R., 2016. A web resource for mining HLA associations with adverse drug reactions: HLA-ADR. Database. (Oxford) 2016.

Gul, A., Ohno, S., 2012. HLA-B*51 and Behçet disease. Ocul. Immunol. Inflamm. 20, 37–43.

He, X.J., Jian, L.Y., He, X.L., Wu, Y., Xu, Y.Y., Sun, X.J., Miao, L.Y., Zhao, L.M., 2013. Association between the HLA-B*15:02 allele and carbamazepine-induced Stevens-Johnson syndrome/toxic epidermal necrolysis in Han individuals of northeastern China. Pharmacol. Rep. 65, 1256–1262.

Hentzien, M., Cuzin, L., Raffi, F., Jacomet, C., Reynes, J., Rey, D., Ravaux, I., Cheret, A., Viguier, M., Bani-Sadr, F., Dat'AIDS study group, 2020. Factors associated with psoriasis in a French Nationwide HIV cohort: the independent role of HLA-B*57:01. AIDS. 34, 1057–1063.

Hu, F.Y., Wu, X.T., An, D.M., Yan, B., Stefan, H., Zhou, D., 2011. Pilot association study of oxcarbazepine-induced mild cutaneous adverse reactions with HLA-B*1502 allele in Chinese Han population. Seizure. 20, 160–162.

Hung, S.I., Chung, W.H., Liu, Z.S., Chen, C.H., Hsih, M.S., Hui, R.C., Chu, C.Y., Chen, Y. T., 2010. Common risk allele in aromatic antiepileptic-drug induced Stevens-Johnson syndrome and toxic epidermal necrolysis in Han Chinese. Pharmacogenomics. 11, 349–356.

Illing, P.T., Vivian, J.P., Dudek, N.L., Kostenko, L., Chen, Z., Bharadwaj, M., Miles, J.J., Kjer-Nielsen, L., Gras, S., Williamson, N.A., Burrows, S.R., Purcell, A.W., Rossjohn, J., McCluskey, J., 2012. Immune self-reactivity triggered by drug-modified HLA-peptide repertoire. Nature. 486, 554–558.

Illing, P.T., Pymm, P., Croft, N.P., Hilton, H.G., Jojic, V., Han, A.S., Mendoza, J.L., Mifsud, N.A., Dudek, N.L., McCluskey, J., Parham, P., Rossjohn, J., Vivian, J.P., Purcell, A.W., 2018. HLA-B57 micropolymorphism defines the sequence and conformational breadth of the immunopeptidome. Nat. Commun. 9, 4693.

Jaruthamsophon, K., Tipmanee, V., Sangiemchoey, A., Sukasem, C., Limprasert, P., 2017. HLA-B*15:21 and carbamazepine-induced Stevens-Johnson syndrome: pooled-data and in silico analysis. Sci. Rep. p. 7, 45553.

Kongpan, T., Mahasirimongkol, S., Konyoung, P., Kanjanawart, S., Chumworathayi, P., Wichukchinda, N., Kidkeukarun, R., Preechakul, S., Khunarkornsiri, U., Bamrungram, W., Supharatwattanakun, B., Mootsikapun, P., Kwangsukstid, S., Denjanta, S., Vannaprasaht, S., Rungapiromnan, W., Suwankesawong, W., Tassaneeyakul, W., 2015. Candidate HLA genes for prediction of co-trimoxazole-induced severe cutaneous reactions. Pharmacogenet. Genomics 25, 402–411.

Loll, B., Fabian, H., Huser, H., Hee, C.S., Ziegler, A., Uchanska-Ziegler, B., 2016. Increased conformational flexibility of HLA-B*27 subtypes associated with ankylosing spondylitis. Arthritis Rheum. 68, 1172–1182.

Martin, A.M., Nolan, D., Gaudieri, S., Almeida, C.A., Nolan, R., James, I., Carvalho, F., Phillips, E., Christiansen, F.T., Purcell, A.W., McCluskey, J., Mallal, S., 2004. Predisposition to abacavir hypersensitivity conferred by HLA-B*5701 and a haplotypic Hsp70-Hom variant. Proc. Natl. Acad. Sci. U. S. A. 101, 4180–4185.

Martin, A.M., Almeida, C.A., Cameron, P., Purcell, A.W., Nolan, D., James, I., McCluskey, J., Phillips, E., Landay, A., Mallal, S., 2007. Immune responses to abacavir in antigen-presenting cells from hypersensitive patients. AIDS. 21, 1233–1244.

Mockenhaupt, M., Wang, C.W., Hung, S.I., Sekula, P., Schmidt, A.H., Pan, R.Y., Chen, C. B., Dunant, A., Gouvello, S.L., Schumacher, M., Valeyrie-Allanore, L., Bellon, T., Kardaun, S.H., Jan, Y.S., Chung, W.H., Roujeau, J.C., group, R, 2019. HLA-B*57:01 confers genetic susceptibility to carbamazepine-induced SJS/TEN in Europeans. Allergy. 74, 2227–2230.

Morishima, N., 2005. Control of cell fate by Hsp70: more than an evanescent meeting. J. Biochem. 137, 449–453.

Ostrov, D.A., Grant, B.J., Pompeu, Y.A., Sidney, J., Harndahl, M., Southwood, S., Oseroff, C., Lu, S., Jakoncic, J., de Oliveira, C.A., Yang, L., Mei, H., Shi, L., Shabanowitz, J., English, A.M., Wriston, A., Lucas, A., Phillips, E., Mallal, S., Grey, H.M., Sette, A., Hunt, D.F., Buus, S., Peters, B., 2012. Drug hypersensitivity caused by alteration of the MHC-presented self-peptide repertoire. Proc. Natl. Acad. Sci. U. S. A. 109, 9959–9964.

Pan, R.Y., Dao, R.L., Hung, S.I., Chung, W.H., 2017. Pharmacogenomic advances in the prediction and prevention of cutaneous idiosyncratic drug reactions. Clin. Pharmacol. Ther. 102, 86–97.

Perria, C.L., Rajamanickam, V., Lapinski, P.E., Raghavan, M., 2006. Catalytic site modifications of TAP1 and TAP2 and their functional consequences. J. Biol. Chem. 281, 39839–39851.

Phillips, E., Bartlett, J.A., Sanne, I., Lederman, M.M., Hinkle, J., Rousseau, F., Dunn, D., Pavlos, R., James, I., Mallal, S.A., Haas, D.W., 2013. Associations between HLA-DRB1*0102, HLA-B*5801, and hepatotoxicity during initiation of nevirapine-containing regimens in South Africa. J. Acquir. Immune Defic. Syndr. 62, e55–e57.

Queiro, R., Morante, I., Cabezas, I., Acasuso, B., 2016. HLA-B27 and psoriatic disease: a modern view of an old relationship. Rheumatol. (Oxf. Engl.). 55, 221–229.

Rizvi, S.M., Salam, N., Geng, J., Qi, Y., Bream, J.H., Duggal, P., Hussain, S.K., Martinson, J., Wolinsky, S.M., Carrington, M., Raghavan, M., 2014. Distinct assembly profiles of HLA-B molecules. J. Immunol. 192, 4967–4976.

Roe, D.R., Cheatham, T.E., 2013. PTRAJ and CPPTRAJ: software for processing and analysis of molecular dynamics trajectory data. J. Chem. Theor. Comput. 9, 3084–3095.

Saag, M., Balu, R., Phillips, E., Brachman, P., Martorell, C., Burman, W., Stancil, B., Mosteller, M., Brothers, C., Wannamaker, P., Hughes, A., Sutherland-Phillips, D., Mallal, S., Shaefer, M., 2008. Study of hypersensitivity to a, Pharmacogenetic evaluation study T: high sensitivity of human leukocyte antigen-b*5701 as a marker for immunologically confirmed abacavir hypersensitivity in white and black patients. Clin. Infect. Dis. Off. Publ. Infect. Dis. Soc. Am. 46, 1111–1118.

Shirayanagi, T., Aoki, S., Fujimori, S., Watanabe, K., Aida, T., Hirasawa, M., Kumagai, K., Hoshino, T., Ito, K., 2020. Detection of Abacavir-induced structural alterations in human leukocyte antigen-B*57:01 using phage display. Biol. Pharm. Bull. 43, 1007–1015.

Susukida, T., Aoki, S., Kogo, K., Fujimori, S., Song, B., Liu, C., Sekine, S., Ito, K., 2018. Evaluation of immune-mediated idiosyncratic drug toxicity using chimeric HLA transgenic mice. Arch. Toxicol. 92, 1177–1188.

Susukida, T., Kuwahara, S., Song, B., Kazaoka, A., Aoki, S., Ito, K., 2021. Regulation of the immune tolerance system determines the susceptibility to HLA-mediated abacavir-induced skin toxicity. Commun. Biol. 4, 1137.

Taurog, J.D., Dorris, M.L., Satumtira, N., Tran, T.M., Sharma, R., Dressel, R., van den Brandt, J., Reichardt, H.M., 2009. Spondylarthritis in HLA-B27/human beta2-microglobulin-transgenic rats is not prevented by lack of CD8. Arthritis Rheum. 60, 1977–1984.

Tsai, W.C., Chen, C.J., Yen, J.H., Ou, T.T., Tsai, J.J., Liu, C.S., Liu, H.W., 2002. Free HLA class I heavy chain-carrying monocytes–a potential role in the pathogenesis of spondyloarthropathies. J. Rheumatol. 29, 966–972.

Tysoe-Calnon, V.A., Grundy, J.E., Perkins, S.J., 1991. Molecular comparisons of the beta 2-microglobulin-binding site in class I major-histocompatibility-complex alpha-chains and proteins of related sequences. Biochem. J. 277, 359–369.

Wu, X., Wu, J., Li, X., Wei, Q., Lv, Q., Zhang, P., Zheng, X., Chen, Z., Cao, S., Tu, L., Gu, J., 2020. The clinical characteristics of other HLA-B types in Chinese ankylosing spondylitis patients. Front. Med. (Lausanne). 7, 568790.

Wycisk, A.I., Lin, J., Loch, S., Hobohm, K., Funke, J., Wieneke, R., Koch, J., Skach, W.R., Mayerhofer, P.U., Tampé, R., 2011. Epstein-Barr viral BNLF2a protein hijacks the tail-anchored protein insertion machinery to block antigen processing by the transport complex TAP. J. Biol. Chem. 286, 41402–41412.

Yun, J., Cai, F., Lee, F.J., Pichler, W.J., 2016. T-cell-mediated drug hypersensitivity: immune mechanisms and their clinical relevance. Asia Pac. Allergy. 6, 77–89.